Annals of Emerging Technologies in Computing (AETiC)
Vol. 7, No. 5, 2023

Research Article

Chest X-Ray Image Annotation based on Spatial Relationship Feature Extraction

Mohd Nizam Saad[1,*], Mohamad Farhan Mohamad Mohsin[2], Hamzaini Abdul Hamid[3] and Zurina Muda[4]

[1,2]School of Multimedia Technology and Communication, Universiti Utara Malaysia, Malaysia
nizam@uum.edu.my; farhan@uum.edu.my
[3]Department of Radiology, Hospital Canselor Tuanku Muhriz UKM, Malaysia
drzanid@yahoo.com
[4]Faculty of Information Science and Technology, Universiti Kebangsaan Malaysia, Malaysia
zurina@ftsm.ukm.my
*Correspondence: nizam@uum.edu.my

Received: 1st September 2022; Accepted: 5th May 2023; Published: 5th October 2023

Abstract: Digital imaging has become an essential element in every medical institution. Therefore, medical image retrieval such as chest X-ray (CXR) must be improved via novel feature extraction and annotation activities before they are stored into image databases. To date, many methods have been introduced to annotate medical images using spatial relationships after these features are extracted. However, the annotation performance for each method is inconsistent and does not show promising achievement to retrieve images. It is noticed that each method is still struggling with at least two big problems. Firstly, the recommended annotation model is weak because the method does not consider the object shape and rely on gross object shape estimation. Secondly, the suggested annotation model can only be functional for simple object placement. As a result, it is difficult to determine the spatial relationship feature after they are extracted to annotate images accurately. Hence, this study aims to propose a new model to annotate nodule location within lung zone for CXR image with extracted spatial relationship feature to improve image retrieval. In order to achieve the aim, a methodology that consists of six phases of CXR image annotation using the extracted spatial relationship features is introduced. This comprehensive methodology covers all cycles for image annotation tasks starting from image pre-processing until determination of spatial relationship features for the lung zone in the CXR. The outcome from applying the methodology also enables us to produce a new semi-automatic annotation system named CHEXRIARS which acts as a tool to annotate the extracted spatial relationship features in CXR images. The CHEXRIARS performance is tested using a retrieval test with two common tests namely the precision and recall (PNR). Apart from CHEXRIARS, three other annotation methods that are object slope, object projection and comparison of region boundaries are also included in the retrieval performance test. Overall, the CHEXRIARS interpolated PNR curve shows the best shape because it is the closest curve approaching the value of 1 on the X-axis and Y-axis. Meanwhile the value of area under curve for CHEXRIARS also revealed that this system attained the highest score at 0.856 as compared to the other three annotation methods. The outcome from the retrieval performance test indicated that the proposed annotation model has produced outstanding outcome and improved the image retrieval.

Keywords: ***Chest X-ray; Feature extraction; Image annotation; Retrieval test; Spatial relationship features***

1. Introduction

Advanced imaging technology allowed many medical images to be produced on a daily basis. According to a report by the Ministry of Health Malaysia[1], at the end of 2011, there were 151 clinics offering radiology services to patients. In 2012, the number of clinics offering radiology services increased to more than 166 clinics (an increase of 9.9%). Meanwhile, in 2011, a total of 466,583 X-ray examinations were

[1] http://vlib.moh.gov.my/cms/content.jsp?id=com.tms.cms.document.Document_2e692ffb-a0188549-d5315d00-3032d623

Mohd Nizam Saad, Mohamad Farhan Mohamad Mohsin, Hamzaini Abdul Hamid and Zurina Muda, "Chect X-Ray image annotation based on spatial relationship feature extraction ", *Annals of Emerging Technologies in Computing (AETiC)*, Print ISSN: 2516-0281, Online ISSN: 2516-029X, pp. 71-89, Vol. 7, No. 5, 5th October 2023, Published by International Association for Educators and Researchers (IAER), DOI: 10.33166/AETiC.2023.05.007, Available: http://aetic.theiaer.org/archive/v7/v7n5/p7.html.

conducted on patients but the value has increased by 572,532 in 2012 (an increase of 22.7%). Based on these values, it is clear that the development of imaging technology in Malaysia has grown rapidly during the previous decade.

The ability to produce medical images should also be in line with the development of imaging technology as the number of patients who need to seek treatment at health centers are also increasing. Health facts reports from the related ministry depicted that in 2015 alone; for government hospitals alone, there were over 2.4 million patients admitted to wards while a total of 19.9 million people received outpatient treatment at those hospitals[2]. The same source also showed a high number of patients, namely 1.1 million people were admitted to wards in private hospitals while a total of 4 million patients received outpatient treatment in the same type of hospital. The numbers shown do not include patients receiving various other treatments such as dentistry, rehabilitation and maternity. With the increase every year, then the dependence on medical imaging technology is becoming higher. Of course, developments in imaging technology have a very good impact on the health care of the population. Nevertheless, it also presents a major challenge to manage the medical image well. There are various ways that should be explored to launch image management on a large scale such as fast and accurate image search methods, smooth image navigation as well as systematic image storage methods. With efficient image management, the process of storing and accessing images can be done more efficiently.

There are many studies conducted related to managing large medical image repositories efficiently. One of the methods that are interested to explore is the image annotation in order to improve image retrieval. Image annotation is a method of combining (also giving meaning, labeling, marking or indexing) keywords in the form of text on an image to describe the image, improve retrieval and most importantly reduce the semantic gap that exists between low -level and high -level image features [1–3]. The method is proposed in order to reduce the difference between low-level image features and high-level image features which is referred to as semantic gap [4]. In brief, low-level image features such as color, shape and texture are properties used by a computer to recognize an image. Meanwhile for humans, the introduction to an image should be done based on the language they used or known as high level image features. The gap occurred because the low-level image features cannot help the retrieval process as there are users who are not proficient in using these features in the query language created [5]. The situation becomes even critical if the treatment case report does not match every feature of the medical image analysis made [6]. In this situation, the developed retrieval system faces two constraints; firstly, the system is unable to interpret the image content accurately and secondly; the system lacks understanding of the real needs of users [7]. Therefore, image annotation based on high level features is required so that it assists users in the image query hence making the retrieval process efficient.

In computer aided diagnosis field, image annotation using high-level image features has been used for various purposes such as image classification based on shape for X-Ray image to facilitate image management improving image presentation in retrieval systems using the textual similarity of diagnosis reports and describing the location of anomalies detected in medical images [6], [8-9]. Although image annotation has been widely used, there is still lack of research that exploits spatial position and its relationship to describe pixels, objects or regions in images [10-11]. This situation occurs due to the difficulty in assigning appropriate keywords to words or phrases in actual sentences to state the spatial relationship among objects in these images [12].

To date there are at least three methods for annotating images using spatial relationship features and are suitable to be implemented for medical images namely object slope [13-14], object projection [15-16] and region boundaries [17]. However, one common problem occurring in each method is that the model used to determine the spatial relationship features between the main object and its reference is still weak and inefficient. Additionally, the model formed sometimes does not take into account the shape of the reference objects to determine the direction of the spatial relationship, instead it only makes rough object estimation which is summarized in the form of points or slopes [18]. As a result, extra processes such as spatial reasoning using a set of spatial rules are required to determine the spatial relationships features. Moreover, some proposed models only work for simple object position structures i.e. only one component of the object is connected and does not have complex object structures such as holes [19]. Whereas in the real situation,

[2] https://www.moh.gov.my/moh/images/gallery/Report/Country_health.pdf

the structures of objects are very complex with holes, polygonal shape and may intersect among each other in the medical images. For this reason, the direction of the spatial relationship becomes very challenging due to the rapidly changing in Cartesian polarity. In short, annotating medical images with spatial relationship features is very complex and challenging. However, if this challenge can be simplified then it will be a great opportunity because one should note that spatial relationship is a high level image feature that is easily identifiable by the user. The usage of this feature improves image retrieval hence researchers should take the opportunity to use this feature to annotate medical images. Therefore, this paper discussed our experience building an image annotation model based on spatial relationship feature extraction to improve image retrieval. The model annotates the location of nodules in the lung zone for chest X-Ray (CXR) images using spatial relationship features. Annotated images with the extracted features improved the retrieval from the image repository.

2. Image Annotation

Rapid technology evolution over the past two decades has successfully increased the importance of visual data in parallel with textual. As a result, the requirements to acquire an effective and efficient form of tool for manipulating visual information has become increasingly important. In order to meet this need, researchers have been proposing image retrieval techniques by annotating image files using visual image features as a solution. Figure 1 displays the visual space, the semantic space and the textual space which contribute the basic process of image annotation as found in [20].

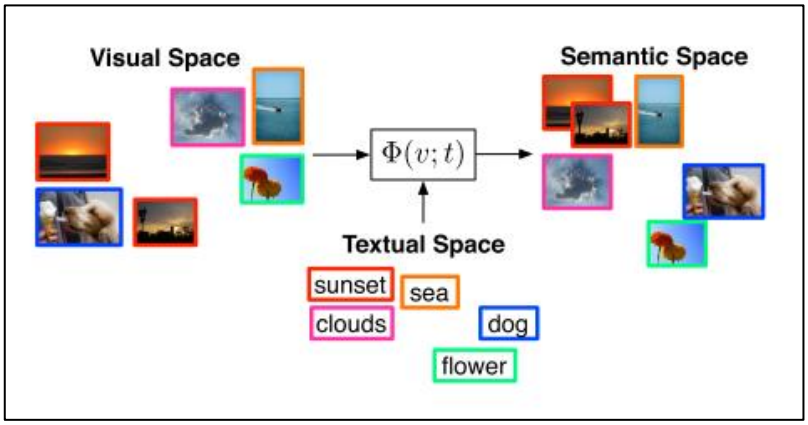

Figure 1. Visual space, semantic space and textual space for the annotation process

In Figure 1, the input images have visual space that can be interpreted uniquely according to the person who is viewing it. Everyone has their own perception to give visual meaning according to their point of view. This point of view also provides a meaning also known as semantics (or semantic space) for defining the visual of the image. Meanwhile in the annotation process, this semantic space will be used as keywords such as sunset, sea, clouds etc. to give meaning to the visual form of the image.

In general, these methods can be divided into three approaches namely traditional annotation, content based image retrieval (CBIR) and automatic image annotation (AIA) [21]. In the first approach, one would annotate the image manually then retrieve the image by linear search according to keywords such as the method of acquiring a text document. This method is simple however it is not practical if it involves large amounts of images because human-made annotation methods are often very subjective and too vague [22]. The second approach is focused on CBIR with each image indexed and retrieved automatically using low-level image features such as color, shape and texture [23–25]. Although the latter approach is effective in increasing the percentage accuracy of finding images from the repository, researchers found that reliance on low-level image properties widens the semantic gap between humans and computer systems.

Since the first and second method approaches have limitations to provide a good form of image retrieval tool then some researchers introduced a third approach known as AIA. Technically, AIA or also known as auto-annotation or linguistic indexing [26] is a task to add descriptive text features to an image to increase the semantic value of the image [27].The main goal of adding a descriptive label to an area or object in an image is to present its semantic content as a short step to more effective image search and retrieval. Apart from visual data-based access, annotated areas or objects can also be searched based on text.

3. Spatial Relationship Image Feature

One of the objectives from previous researchers for introducing CBIR was to facilitate the retrieval of images found in image databases [28]. In fulfilling this facility, they used features found on the image as the input to retrieve the similar images. Basically, there are two types of image features commonly used as inputs in CBIR namely visual features and spatial features. Retrieving images using spatial relationship features refers to a method for determining the location of an object in an image as well as its relationship with other objects [21], [29]. Spatial relationship is a form of relationship that is uncertain or fuzzy and it depends on an individual to determine exactly the true form of relationship [15], [30]. According to [31], there are two ways to present the spatial relationship between objects that is through topological relationship and directional relationship. In both relationships, the spatial relationship features should be used to form a complete relationship between objects. To get a clearer picture of the features of spatial relationships, the next subsection discusses these features, especially the use of spatial relationship features in determining topological and directional spatial relationships.

3.1. Topological Spatial Relationship Features

Spatial relationship features in this category are used to produce relationships between objects whose relationships do not change despite topological transformations [31–33]. Intended changes include processes such as changing the position objects, scaling the objects size or changing the position such as changing the coordinates of a reference object. In most studies related to topological spatial relationship features, it was found that the most frequent model used to present this relationship is the region connection calculus (RCC-8) model [34–36]. In the RCC-8 model, there are eight topological spatial relationship features that are highlighted to describe the relationship of objects in a space that is disconnected (DC), externally connected (EC), equal (EQ), overlapping, partially overlapping (PO), tangential proper part (TPP), inverse tangential proper part (TPP^{-1}), without complete tangential part (NTPP) and without a non-tangential proper inverse part ($NTPP^{-1}$). Figure 2 shows the eight topological spatial relationship features used in the RCC-8 model.

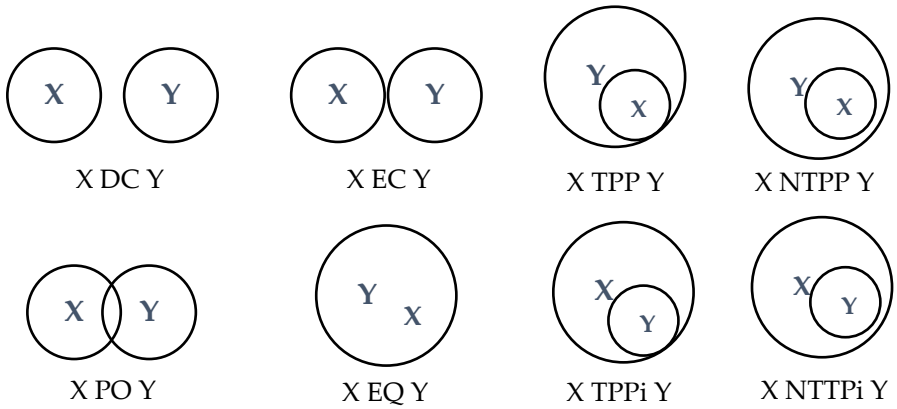

Figure 2. Eight topological spatial relationship features

In Figure 2, the relationship of two objects namely object X and object Y is used as an example to illustrate the use of topological spatial relationship features. In every topological relationship between these objects, object boundaries are used as a mechanism to determine the spatial relationship. Although the spatial relationship features used in the RCC8 model are very effective in showing relationships between objects, the terms used to describe such features are difficult to understand. For instance, relationships involving an object inside another object such as the non-tangential proper part are difficult to understand and to illustrate. Therefore, some researchers prefer to use simple spoken language to describe the spatial relationships such as the term contain or contained to describe an object being inside another object or other terms such as cover and covered by to describe the state of an object in another object. These terms are much easier to understand and assist the process of spatial reasoning among objects.

3.2. Directional Spatial Relationship Features

Directional spatial relationship features are formed based on the relative position between objects according to their current direction [37]. The directional spatial relationship features are derived depending on part or entire orientation of the reference and the main object. This means that if one of the objects changes (such as size reduction or rotation) then the orientation of the two objects also changes, causing modification in the relationship between the objects.

The directional spatial relationship features can be presented using at least two models such as the cone-shaped model and the projection model [35]. In both models, directional spatial relationship features are presented using eight cardinal directions that are typically indicated in compass directions namely north, northeast, east, southeast, south, southwest, west, and northwest. Figure 3(a) shows the cone shape model while Figure 3(b) shows the projection model.

(a) Cone-shaped model (b) Projection model

Figure 3. The cone and projection model

Apart from using the eight cardinal directions for the directional relations, there are researchers who use directions that are more easily understood to indicate the direction of object position. For example, the term for north direction is replaced by upper, higher and peak while the south direction is replaced by below or lower [38-39]. Meanwhile, a combination of two directions is used to replace the intermediate direction i.e. top-right replaces northeast, top-left replaces southwest, bottom-right replaces southeast and bottom-left replaces southwest.

4. Image Annotation Based On Spatial Relationship Feature Extraction

There are at least three methods introduced to annotate objects with spatial relationship features namely object slope, object projection and regional boundary comparison. The purpose of the discussion for all stated annotation methods is to compare each of these methods.

4.1. Image Annotation Based On Object Slope

Slope refers to the estimate of the inclination over the degree of rotation on a straight line in a column In studies involving direction determination, slope elements are used to determine the hill slope direction, wind direction, river flow and cloud movement direction [15]. According to [13], there are two forms of slope, namely incline slope or positive slope and decline slope or negative slope. An incline slope occurs when the degree of slope is smaller than the right angle (90^0), while a decline slope occurs when the degree of slope is bigger than the right angle. Slope values are calculated using two methods namely trigonometry and geometry [40].

There are three main components in the calculation of angles for trigonometry namely sine, cosine and tangent. In [13], tangents have been used to obtain the slope angle. In Figure 4, given two objects namely Object 1 and Object 2 as well as a triangle ABC. To calculate the degree of slope θ, equation (1) is used:

$$\theta = \tan^{-1}\left(\frac{AB}{AC}\right) \quad (1)$$

In formula 1, the degree of slope θ is calculated using the inverse tangent of the distance from the line AB relative to the distance of the line AC. Based on the degree of slope obtained, the direction of the spatial relationship between the two objects is determined.

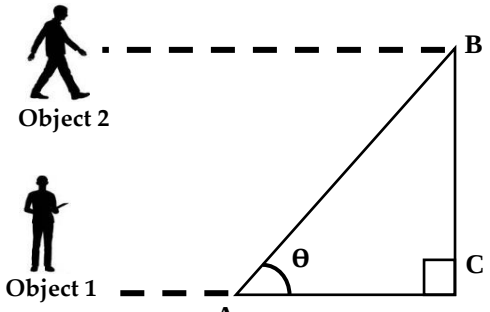

Figure 4. Slope calculation using trigonometry

Meanwhile the geometry-based slope calculation is much simpler as it requires only two coordinate points where the slope value is determined by distinguishing the coordinate point on the high Y-axis versus the low Y-axis coordinate point [41](see Figure 5 as illustrated in [42]).

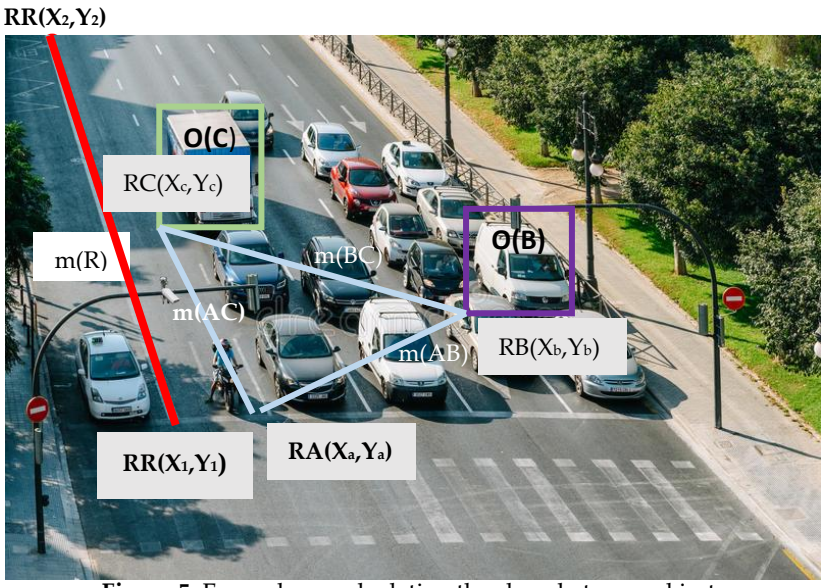

Figure 5. Example on calculating the slope between objects

The slope calculation is simple because only one point from the minimum boundary rectangle (MBR) of the object is needed to represent the whole object. In Figure 5, each object is represented by an individual MBR, while each MBR is represented by a coordinate point located on the diagonal of each MBR. For example, the bottom-left diagonal coordinates of object A (O (A)) are represented by RA (Xa, Ya), the coordinate representation of object B (O (B)) is RB (Xb, Yb) and the coordinate representation of object C (O (C)) is RC (Xc, Yc). In order to obtain the slope between two objects, differences between the coordinate values on the same axis are calculated so that the slope value is derived. According to [42], the equation to calculate the slope of object 1 and object 2 (m12) is as follows:

$$\text{Slope of object 1 and object 2} = \text{m}\ (12) = \frac{Y_2 - Y_1}{|X_2 - X_1|} \quad (2)$$

For instance, let two points; A and B with coordinates of (1,6) and (5,3) respectively. Then the slope for object A and B is 2 based on Formula 2.

$$\text{m}\ (\text{AB}) = \frac{3-1}{|5-6|} = 2$$

Since the reference point for calculating the slope guided by the MBR is too dynamic and vary easily due to changes in the Cartesian polarity, then the determination of the spatial relationship for two objects is made using a set spatial rules set such as follow:

If:

m (AB)> 0, A in front of B

m (AB) <0, A behind B
m (AB) = ∞, A in front/behind B
m (AB) = 0, A on the left/right to B

These spatial rules do not limit binary relations for annotated objects, instead the rules also can be expanded so that it allows for multiple relations. Based on slope values, the spatial rules have the advantage of identifying relationships at the vertical positions (front and behind). The rules for vertical position also can be modified to identify top and bottom relationships. However, these rules present little difficulty in identifying the relationship at the horizontal position because the determination for the left or right spatial relationship is vague (the slope value is assumed to be zero). Ideally, a non-zero value should be assigned to the horizontal position rules so that the spatial relationship of either left or right objects can be finite.

4.2. Image Annotation Based On Object Projection

The object projection is an annotation method to determine the direction of the spatial relationship for the main object and its reference object using directional relations [43], [44]. With this method, the position of the main object is determined by projecting its position based on the reference object. To determine the direction of an object, a cluster of projection regions is applied around the reference object by dividing the area around the reference object into nine regions according to a 3x3 matrix [33], [45] as shown in Figure 6.

Figure 6. Example for determine the spatial relationships for object projection methods

These nine projection regions are known according to the cardinal direction while the central region is known as neutral zero [18]. Based on each projection region cluster, the position of the main object is decided once it intersects with one of the nine projection regions. In Figure 6, there are two objects marked with O(R); the reference object and O(M); the main object. Using the object projection method, nine projection regions are generated around the reference object. The position for both objects are determined based on the intersection of the main object with the projection region produced around the reference object. A relationship can be written as D(A, B) which carries the meaning of direction for object A to B respectively. Meanwhile, in order to decide the actual direction of the reference object to the main object, the calculation for percentage area of intersection can be done to indicate how large the main object intersects the projection region. The percentage value would definitely determine the direction between the reference object to the main object. The relationship between the reference object and the main object can be simplified as D(O(R), O(U)) = northeast or it meant that the direction of the reference object to the main object is northeast.

Although the method for obtaining the spatial relationship with the object projection seems convincing, it has some drawbacks. Firstly, the process of producing the projection region would be difficult if the shape of the object is complex (such as a polygon). Secondly, even if the projection region is successfully formed, other problems might arise such as main objects and references intersecting with each other in the image. Thirdly, if the positions of the main and the reference object do not intersect at all, the way to determine the spatial relationship is still challenging because the total combination of cardinal directional relationships

for a set of regions can exceed up to 511 relationship elements. Therefore, all issues need special attention in order to select this method to annotate images with spatial relationship features.

4.3. Image Annotation Based On Comparison of Region Boundaries

The comparison of region boundaries was introduced to annotate the absolute and the relative object position in pairs with other objects [29]. Based on these two positions, the position of the main object and its relative position to the reference object can be known. Thus, the main object can be annotated with the appropriate spatial relationship features. To implement this method, an object needs to be segmented from the original image and then labelled with an appropriate description [46-47]. Each object that goes through both processes can be identified based on the pixel coordinate that covers the object boundary and the additional label assigned to describe the object. For instance, assuming that an object is segmented from an image then the representation of the object can be done using collection of pixel coordinates surrounding the object's boundary which referred as follows i.e. coordinates for Object 1 = {(x1, y1), (x2, y2),…, (xn, yn)} , coordinates for object 2 = {(x1, y1), (x2, y2),…, (xn, yn)} and object coordinates for object N = {(x1, y1), (x2, y2),…, (xn, yn)}.

To begin the annotation process, the average coordinates of the X-axis and Y-axis found around the region boundary need to be calculated to obtain the midpoint of gravity or centroid. Next, comparison of one object position with another object is performed using the centroid because this point represents the region. The usage of centroid in this method has many advantages such as a point to represent the region, determinant point for region location and markers for calculating radius, width and angle of an object. Based on the obtained centroid coordinates, the position comparisons between pairs of objects are determined using a set of spatial rules. Similar to the object projection annotation method, the spatial location between each object is determined either using cardinal direction or basic direction indicators (left, right, etc.). Figure 7 shows an example to determine the type of spatial relationship between two objects using the comparison of regional boundaries. In the figure, the determination of the spatial relationship between two objects begins by estimating the MBR for each object. Next, the centroid of the object is obtained by calculating the average of coordinate points surrounding the MBR. Apart from the centroid, the MBR height is also used as a spatial entity to determine the spatial relationship. Some researchers calculate the MBR width to set it as part of the entity for the object to determine the spatial relationship. Finally, once all spatial entities are acquired, a set of spatial rules is used to compare and determine the most appropriate type of spatial relationship for the objects pairs.

Annotation based on the region boundary is simple because it relies only on information obtained from centroid and the MBR height; however, the usage of centroid point has limitations. Firstly, centroid is not precise because this coordinate only represents one pixel in the object region. Secondly, the usage of centroid points has resulted in the determination of cardinal directional does not take into account other important object's entities such as shape and area. Third, since only the coordinates of the centroid are used as spatial entities, deriving spatial relationship features is difficult if the main object's centroid overlaps with the reference object centroid. Therefore, image annotation using comparison of region boundaries needs to be refined especially in deciding the centroid so that this entity represents the object accurately.

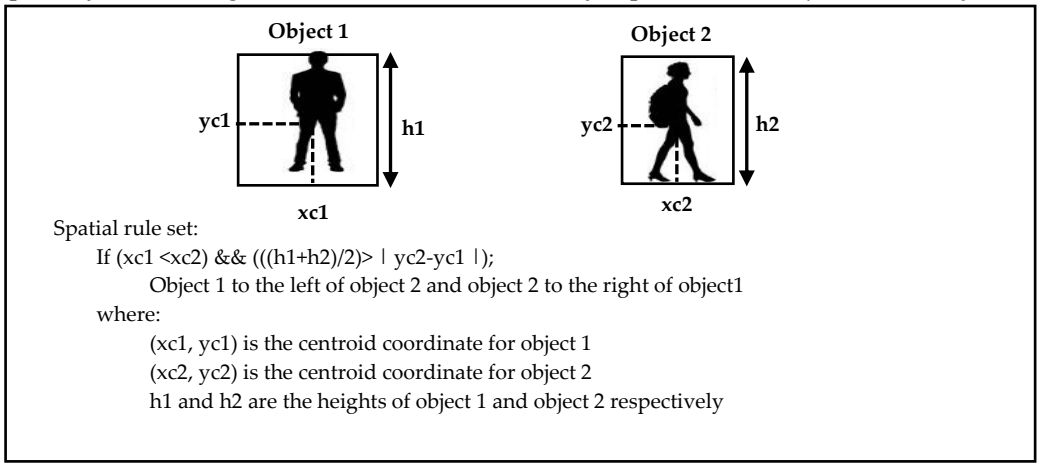

Figure 7. Determination of the spatial relationships for the regional boundary comparison

5. Image Annotation Experiment Using Spatial Relationship Features

In image annotation experiment, six processes were taken to annotate XRD images with spatial relationship features. Figure 8 shows the annotation processes and the component for multi-class image classification using the Support Vector Machine (SVM) to classify annotated images based in the lung nodule location in the lung zones (please refer to [48] for details discussion on image classification).

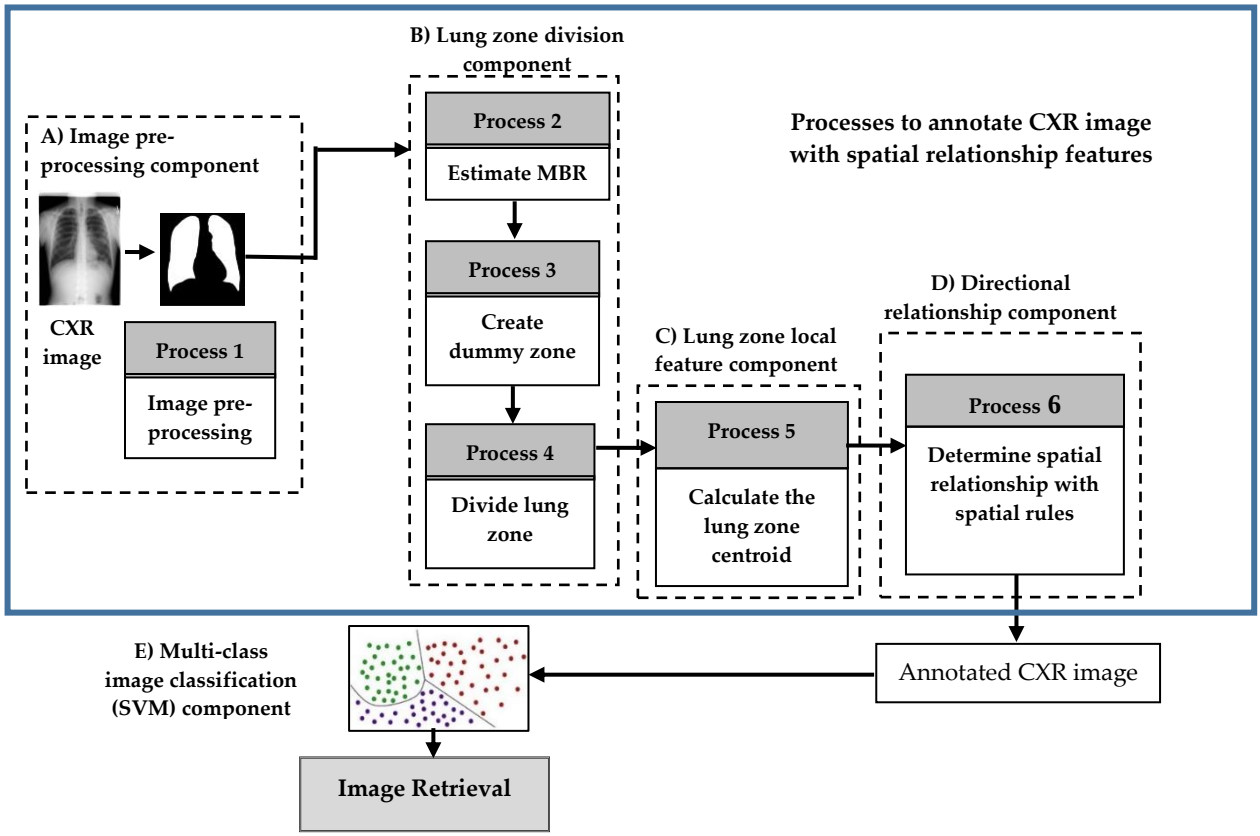

Figure 8. The process flow to annotation CXR image with spatial relationship features

In Figure 8, there are six process performed image annotation which include image pre-processing (segment lung areas from other anatomy), estimate the MBR for the segmented lung area, create a dummy zone between the right and left lungs, divide the lung area into zones (region of interest) according to the features of spatial relationship, calculate the centroid for each zone (referred as the lung zone) and determine the spatial relationship between the nodule location and the lung zone through spatial rules. In Figure 8, the four main components for the image annotation are illustrated in a dotted lines rectangular box. Additionally, during the experiment, we annotate CXR images taken from the Japan Society of Radiological Technology (JSRT).

5.1. Image Pre-Processing

Image pre-processing is a routine process performed to improve image quality so that attributes that degrade the image during the digital imaging process are removed. In this experiment, the image pre-processing component was placed as the first component to be performed on each image before it undergoes the annotation process. For medical images, early image processing is important to improve image appearance where methods like adjusting the image contrast, noise reduction and image rescaled will be performed.

5.2. MBR Estimation for Segmented Lung Area

Once the binary image containing only the lung area is generated from the image segmentation, we run the next step which is to divide the lung area into six zones (as recommended by radiology specialists). This division requires the second component which is the lung zone division component. The initial step in

the division is to produce the lung area MBRs as shown in Figure 9. Since the binary image generated from the image segmentation has only two objects namely the left and right lungs, the process to generate the MBR is straightforward. Using image processing software such as Matlab, the MBR size can be estimated using an anchor point. For each anchor point, four parameters, namely coordinate point for the X-axis, coordinate point for the Y-axis, the MBR width and the MBR height are generated by the software. For example, in Figure 9, suppose T1 is the anchor point for the MBR of the right lung. Thus, the MBR size for the right lung can be estimated based on X-axis coordinate of point T1, Y-axis coordinate of point T1, the MBR width on the X-axis from point T1 and the MBR length on the Y-axis of point T1.

5.3. Dummy Zone for Right and Left Lungs

If we observe the position of the left and right lungs in Figure 9, we will notice that there is an empty space between the both lungs. This space appears because human lungs exist in two pieces i.e. the left and right lung and there is space between them to separate this organ. Although this space is empty yet it is important because it distinguishes the lungs apart from breaking the lung structure. Therefore, in this experiment, this empty space is filled with a dummy zone which is a zone to divide the left and right lungs.

To generate the dummy zone, anchor points and MBRs were used. In addition, four coordinate points representing the dummy zone area are required, namely the left-top and left-bottom diagonal points of the left lung MBR's and the right-top and right-bottom diagonal points of the right lung MBR. Suppose there are two anchor points namely T1 for the right lung and T2 for the left lung.

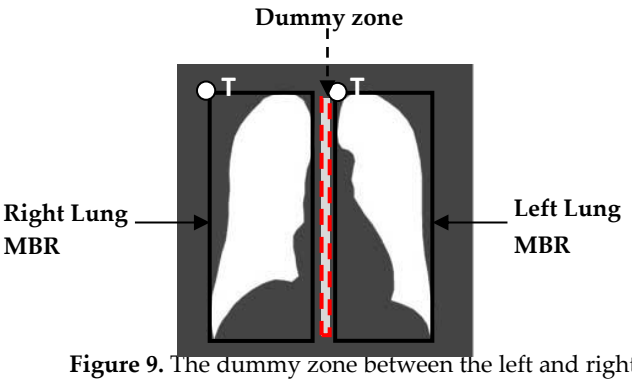

Figure 9. The dummy zone between the left and right lung

Therefore, the right lung MBR parameters can be formulated as x-CoorT1, y-CoorT2, W1 and H1. Here, x-CoorT1 is the T1 coordinate on the X-axis, y-CoorT1 is the T1 coordinate on the Y-axis, W1 and H1 are the width and height of the MBR for the right lung. Using the same method, the MBR parameters for the left lung were x-CoorT2, y-CoorT2, W2 and H2. Since the dummy zone is produced as a square shape, then all the parameters of the zone can be formed in the same way as the MBR. By using all the specified parameters, the desired dummy zone can be formed. It is positioned between the right and left lungs to separate both organs and assist the identification of the lung type.

5.4. Lung Zones Division

We discovered interview sessions with radiology specialist that lung area will be divided into two horizontal zones (left and right) and three vertical zones (top, middle and bottom) (2x3 dimensions) to diagnose lung conditions. Therefore, in the experiment, we adapted the same method to form lung zone. Horizontal zones division is simple because the lungs are indeed divided into two parts namely the left and right lungs. However, three vertical lung zones division are quite bit difficult because the division guidelines are vague. When we referred to the radiologist he replied that in general, the first zone, called the upper zone is above the helium, the lower zone is one-third of the lungs, while the middle zone is one-third in the middle of the lungs. He added that this division is vague due to the lack of accurate division guidelines to refer. After a series of discussions with him, we suggest that the division of the vertical zone can be done based on the height of the dummy zone. This division is made by factoring of the dummy zone into three equal parts. Figure 10 shows our suggestion to divide the lung zones.

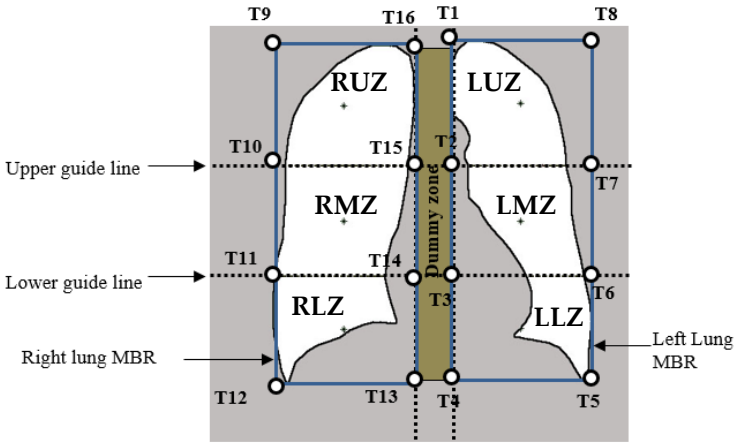

Figure 10. The area division

In order to divide the lung height into three vertical zones based on the dummy zone height, two lines need to be generated namely the upper and the lower guide lines. Meanwhile, it is not sufficient to divide the horizontal division into two zones because the existence of a dummy zone. Hence, we suggest that the horizontal division also need to be divided into three parts, namely the left lung, dummy zone and right lung. With this division method, the lung area is divided into nine zones (3x3 zones) covering three horizontal zones and three vertical zones. In this experiment, we use the same naming convention in radiology to describe each lung zone that are Left Upper Zone (LUZ), Left Middle Zone (LMZ), Left Lower Zone (LLZ), Right Upper Zone (RUZ), Right Middle Zone (RMZ) and Right Lower Zone (RLZ).

5.5. Centroid Point Calculation for Lung Zones

Once every lung zone is successfully divided, the centroid of each zone can be calculated and acted as the local representation for each zone. The calculation to derive the centroid was made using the third component which is the component to present the local features for the lung zone. In order to calculate the centroid, only the lung area within the lung zone was taken into account. Suppose all coordinates covering one lung zone are {(x1, y1), (x2, y2),, (x3, y3),…. (xn, yn)}. Then, the centroid of that lung zones are calculated using equation (3) and equation (4):

$$\mathrm{XCzon} = \min(\mathrm{x1}, \mathrm{x2}, \mathrm{x3},. \mathrm{Xn}) \quad (3)$$

$$\mathrm{YCzon} = \min(\mathrm{y1}, \mathrm{y2}, \mathrm{y3},. \mathrm{Yn}) \quad (4)$$

where XCzon and YCzon are the X-axis and Y-axis coordinates of the centroid for each lung zone.

5.6. Spatial Relationship Determination Through Spatial Rules

When all zones contain the centroid, set of spatial rules to determine the location of nodules in the lung zone can be created. For this purpose, the fourth annotation component which is the directional relationship inference is used. The spatial rules are made based on the spatial relationship features between three entities namely the coordinates of the centroid of the dummy zone, the four points that form the boundary of the dummy zone and the coordinate points of the nodule (taken from the JSRT dataset). During the process of determining the position of a nodule in the lung zone, the coordinates of the nodule need to be identified first before its position in the lung zone is finalized. Later, the classification of the image according to the position of the nodule is executed so that the process to search and retrieve the image would be efficient.

6. Result and Discussion

The image retrieval performance test is performed to evaluate the efficiency of each image annotation method. In the test, we compared our propose method with three annotation methods that are object slope (OS), object projection (OP) and comparison of region boundaries (CoB) (as discussed in Section 4). The main process in the test is to retrieve annotated images from the database. Our proposed image annotation method in the test is known as Chest X-Ray Image Annotation and Retrieval System (CHEXRIAS). CHEXRIAS also contains all components required for image annotation as shown in Figure 8.

Meanwhile, precision and recall (PNR) test was selected as the golden standard for the retrieval performance test. The PNR curve is used because it can determine the retrieval performance based on the skewness of the curve where the skewer the curve to the upper-right corner, the better the performance of the retrieval method. In addition, we also used the area under curve (AUC) value to present the level of accuracy of the image retrieval. The accuracy value obtained enable us to indicate the extent to which a method is able to predict a relevant object from a group of objects (Kozma & Kaski 2009). In addition, Matsakis et al. (2004) stated that the AUC value for the performance of a method can be interpreted as Table 1. Based on the AUC values listed, it is the goal of each retrieval test to achieve the highest AUC value that is close to the value of 1.

Table 1. AUC value and its indicator

AUC Value	Performance indicator
> 0.9	Excellent
> 0.8	Good
> 0.7	Moderate
> 0.6	Weak
< 0.5	Fail

On the other hand, in each retrieval performance test, we used query based on the position of the nodule in the lung zone to get back the annotated imaged. Records of nodule position in the lung zone for all image files were obtained from the dataset provided by JSRT. Briefly, there are three steps performed in the retrieval test:

1) Generate a query to retrieve the image based on the position of the nodule in the lung zone
2) List the image retrieval results based on the query
3) Form a PNR curve from the precision point value and recall

6.1. PNR Curve and AUC for Image Retrieval Test

In the test, we have retrieved images based on the nodule location in the lung for each lung zone. To ease the description for each method performance, we used different colors to represent different annotation methods in the PNR curve. Figure 11 illustrates the all PNR curves and the AUC values for each annotation method (OS, OP, CoB, CHEXRIAS) involving all lung zones.

In the Figure 8, the red curve represents object slope annotation, the green curve represents the object projection annotation, the blur curve represents the comparison of region boundary annotation while the black curve represents CHEXRIAS. This section will elaborate the retrieval performance for each annotation method for every lung zone.

Figure 11(a) shows the PNR curve for the LUZ lung zone for CHEXRIARS and three other image annotation methods. Based on the shape of the PNR curve in the figure, it is found that the OS method shows the best retrieval performance based on its highest position of its PNR curve. The CHEXRIARS and Cob curves are at almost the same position while the object projection curve is at the lowest position. This situation is also confirmed by the AUC value where the AUC value for OS is the highest; 0.910 followed by the CoB and CHEXRIARS of 0.864 and 0.863 respectively. The AUC value for OP is the lowest at only 0.584. In this experiment, the OS obtained the best retrieval performance method because each nodule location located on the right or left lung side in the CXR image would be assumed to be in the LUZ lung zone. The OS method does not have technique to determine the position of the nodule from the middle zone such as the LMZ and LLZ lung zones. Therefore, the method is definitely able to determine all nodule locations in the LUZ lung zone. In this experiment as well, the retrieval performance of CoB and CHEXRIARS is almost the same based on the AUC value obtained. Cob obtained a good AUC value even though it only divided the lung zone into two parts, namely LUZ and LLZ because the location of the nodules at the LUZ position was successfully classified. Nevertheless, in practical terms, the performance of CHEXRIARS is better because CHEXRIARS has divided the lung zone according to the method recommended by the radiologist. Additionally, the CHEXRIARS method successfully retrieved images only from the LUZ lung zone alone without mixing into the LMZ lung zone such as performed by CoB.

(a)

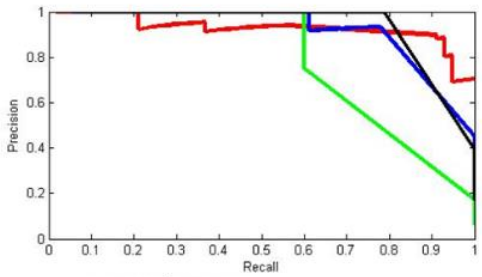

Lung zone = LUZ

Method	AUC value
OS	0.910
OP	0.584
CoB	0.864
CHEXRIARS	0.863

(b)

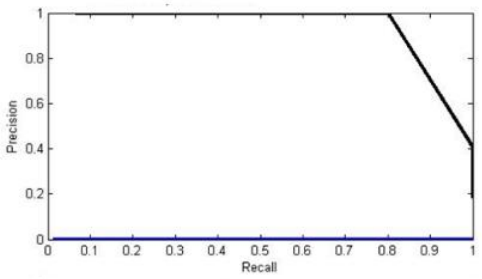

Lung zone = LMZ

Method	AUC value
OS	0
OP	0
CoB	0
CHEXRIARS	0.874

(c)

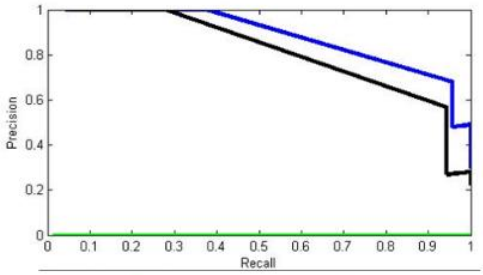

Lung zone = LLZ

Method	AUC value
OS	0
OP	0
CoB	0.842
CHEXRIARS	0.760

(d)

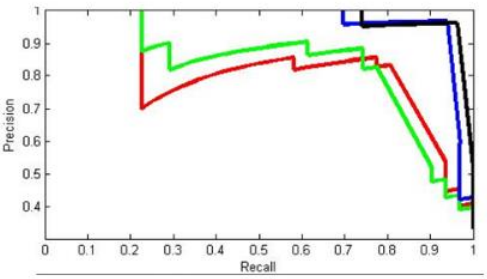

Lung zone = RUZ

Method	AUC value
OS	0.782
OP	0.800
CoB	0.937
CHEXRIARS	0.944

(e)

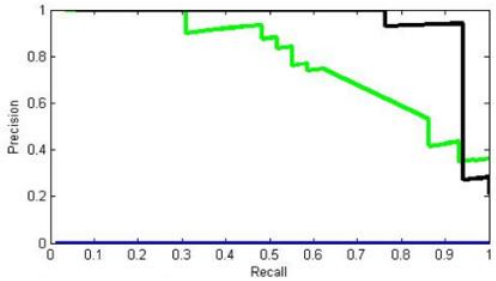

Lung zone = RMZ

Method	AUC value
OS	0
OP	0.754
CoB	0
CHEXRIARS	0.887

(f)

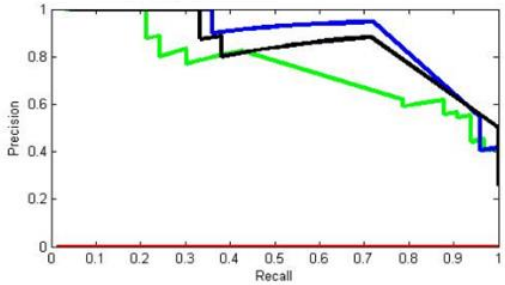

Lung zone = RLZ

Method	AUC value
OS	0
OP	0.732
CoB	0.850
CHEXRIARS	0.808

Figure 11. PNR curve for all lung zones

Figure 11(b) shows the PNR curve for the retrieval test for the LMZ lung zone. Based on the shape of the PNR curve and the AUC values shown in the figure, only CHEXRIARS were able to retrieve images that had nodules in the LMZ lung zone. The PNR curves for the other methods overlap because they are at a constant value on the Y-axis. The AUC values for the three methods were also zero. This condition occurs due to the failure of each of these methods to retrieve images for the LMZ lung zone. From our observation, it was found that the main cause of OS and CoB not succeeding in retrieving the image is because they both do not have a way to form the central lung zone, namely LMZ and RMZ. Additionally, both methods cannot annotate images for the central lung zone such as LMZ. At the same time, it is quite surprising when OP, which has a technique to annotate the image of the central lung zone, fails to retrieve any image in the LMZ lung zone.

Meanwhile, based on the information shown in Figure 11(c), only two methods successfully retrieved the image for the LLZ lung zone namely CoB and CHEXRIARS. Therefore, the figure only shows the PNR curve for the CoB and CHEXRIARS. The PNR curves for OS and OP overlap at constant values on the Y-axis. In the experiments performed, OP failed to classify any image that had nodules location in the LLZ lung zone. The OB, on the other hand, has no way to annotate the LLZ lung zone because the method only shows a way to form annotation in the LUZ zone. Based on the AUC value shown in the same figure, the CoB obtained a higher AUC value at 0.842 compared to CHEXRIARS which managed to get only 0.760. This situation occurs because the CoB has only two zones for the left lung, namely the LUZ and LLZ lung zones. Therefore, image retrieval using CoB can retrieve each image found in the LLZ lung zone. However, there are images that should be classified into the LMZ lung zone but it is considered as the LLZ lung zone using the CoB. In contrast to CHEXRIARS, this annotation system divides the left lung into three lung zones namely LUZ, LMZ and LLZ.

Based on the shape of the PNR curve in Figure 11(d), all methods successfully retrieved images for the RUZ lung zone. In the figure, it is found that the shape of the PNR curve for CHEXRIARS shows the best performance when compared to the others. The shape of the CoB curve shows the second best performance and is followed by the OP and OS curve. Based on the AUC value shown in the figure, it is found that the AUC value obtained by CHEXRIARS is also the highest at 0.944 followed by CoB at 0.937, OP at 0.800 and OS at 0.782. The experimental results show that the performance of CoB and CHEXRIARS is at an excellent level (> 0.9). This condition occurs because both methods have been successful in retrieving images that have the location of nodules in the RUZ lung zone accurately.

Based on the information shown in Figure 11(e), only two methods managed to recover the image for the RMZ lung zone, namely OP and CHEXRIARS. This is because the OS and the CoB have no way of annotating the RMZ lung zone as described in the previous paragraph. Therefore, the figure only shows the PNR curves for OP and CHEXRIARS. In the same figure, the AUC value for CHEXRIARS is higher at 0.887 compared to OP which only obtained 0.754. In this experiment, it was found that for the middle zone annotation method, especially RMZ, for CHEXRIARS it is better than OP. This situation occurs because the way the division involves the area of the central lung zone of CHEXRIARS is better and more accurate.

The last section in Figure 11(f) shows only three methods that successfully retrieved the image for the RLZ lung zone, namely OP, CoB and CHEXRIARS. The OS failed to retrieve image that had a nodule in the RLZ lung zone. Meanwhile, based on the AUC value shown, the AUC value obtained for CoB exceeds the OP and CHEXRIARS which is 0.850 compared to 0.732 and 0.808 respectively. The results shown in the experiments for the RLZ lung zone are almost the same as those obtained in the LLZ lung zone experiments. In both lung zones, Comparison of boundary regions managed to outperform CHEXRIARS. Like the discussion involving the LLZ lung zone, this situation occurs because the CoB has only two zones for the right lung, namely the RUZ and RLZ lung zones. Of course the Comparison of boundary region managed to retrieve each image found in the RLZ lung zone. In fact, there are images that should be classified into the central lung zone which is RMZ but classified as RLZ lung zone.

6.2. Interpolation of PNR Curves

Figure 11 shows the different image retrieval achievements for each lung zone based on the shape of the PNR curve and the AUC value. To facilitate retrieval performance comparison for each method in each lung zone, then a new curve needs to be formed by merging all the existing PNR curves. One of the ways

that can be done to form this new curve is curve interpolation. The interpolation technique helps to calculate the value scattered between several identified points to form a point with a new value [49]. Figure 12 shows four PNR curves and AUC values through interpolation techniques. Each curve shows the average value of precision in addition to the specified recall value.

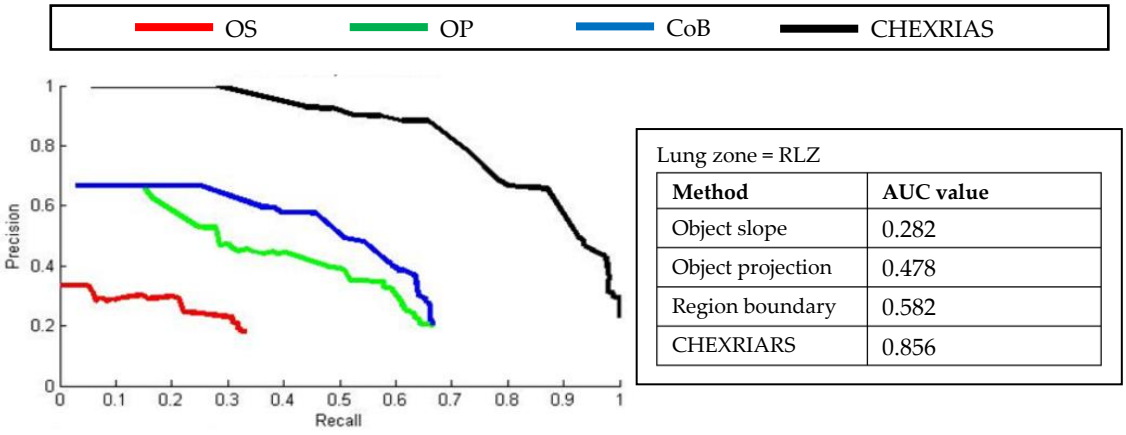

Lung zone = RLZ

Method	AUC value
Object slope	0.282
Object projection	0.478
Region boundary	0.582
CHEXRIARS	0.856

Figure 12. Interpolation PNR curve for all methods

Based on the shape of each new interpolated PNR curve in Figure 12, it is found that the interpolated PNR curve for CHEXRIARS is the best when compared to the interpolated PNR curve of other methods. Only the shape of the interpolated PNR curve for CHEXRIARS is approaching the value of 1 on the X-axis and Y-axis, respectively. The AUC value listed in the figure also shows that the AUC value of CHEXRIARS is the highest at 0.856 followed by the AUC value of CoB of 0. 582, then the AUC value of OP at 0.478 and the AUC value of OS at 0.282. The shape of the interpolated PNR curve and the AUC values confirmed that only CHEXRIARS obtained good retrieval performance (AUC values> 0.8). CoB retrieval performance is weak (AUC value> 0.5) while OS and OP failed in the retrieval experiments conducted (AUC value <0.5). This situation thus indicates that the overall retrieval performance for CHEXRIARS is the best in the retrieval tests conducted.

7. Conclusion

In this paper we discussed our work on CXR image annotation based on spatial relationship feature extraction. Image annotation is very important because it assists the retrieval process from the user query towards the image repository. We proposed six processes that need to be undergone in order to annotate CXR images using the spatial relationship feature. After the image has been annotated, we also conducted a retrieval test for our image annotation system named CXEXRIAS. Based on the retrieval result gained from the test, we found out that CHEXRIARS work well to retrieve images for those with nodules in the right lung zone (RUZ, RMZ and RLZ). This situation is shown through all forms of PNR curves and AUC values for CHEXRIARS in each figure and table involving the right lung zone. Nevertheless, CHEXRIARS were found need to be improved to retrieve images for the left lung zone nodules position especially the LLZ. Although the best retrieval performance was obtained by CHEXRIARS in the LUZ zone while the performance was almost similar for the LMZ, the retrieval performance for the annotation system needs to be improved for the LLZ. To overcome the problem, the method of annotating the image for the left lung especially for the LLZ needs to be revisited. Among the steps that need to be taken is to refine division of lung area into six lung zones and produce a better method to determine the location of nodules that are close to the boundary line between the two lung zones.

In the future we hope that researchers who are interested with our works can improve the following aspect for annotating any types of medical images. First, we want to refine the image segmentation process where we dreamed of creating a more robust image segmentation technique to filter out pixel noise found in CXR images as a result of image manipulation such as image compression and reduction. Secondly, we really would like to test our proposed annotation method with various types of medical images CT scan or perhaps on serial type's medical images such as Magnetic Resonance Imaging (MRI). Third, we also planned to apply the annotation methods to annotate other complex human anatomy such as the brain, blood vessels

and skeletal bones (ribs). With all the proposed future studies, we believe that new findings will be obtained and it will become more useful especially in annotating medical images.

Acknowledgement

This study was supported by the Ministry of Higher Education (MOHE) of Malaysia through Fundamental Research Grant Scheme (FRGS/1/2018/ICT02/UUM/03/1).

References

[1] Pyrros Koletsis and Euripides Petrakis, "SIA: Semantic Image Annotation Using Ontologies and Image Content Analysis", in *Image Analysis and Recognition*, Aurélio Campilho and Mohamed Kamel, Eds. Springer Berlin Heidelberg, ISBN: 978-3-642-13772-3, pp. 374–383, 2010, Published by Springer, DOI: 10.1007/978-3-642-13772-3_38, Available: https://link.springer.com/chapter/10.1007/978-3-642-13772-3_38.

[2] Marcelo Garcia Manzato and Rudinei Goularte, "Automatic Annotation of Tagged Content Using Predefined Semantic Concepts", in *Proceedings of the 18th Brazilian symposium on Multimedia and the web*, São Paulo, Brazil, October 15 – 18, 2012, ISBN: 978-1-4503-1706-1, pp. 237–244, 2012, Published by ACM, DOI: 10.1145/2382636.2382688, Available: https://dl.acm.org/doi/10.1145/2382636.2382688.

[3] Hatem Mousselly Sergieh, Gabriele Gianini, Mario Döller, Harald Kosch, Elöd Egyed-Zsigmond *et al.*, "Geo-based automatic image annotation", in *Proceedings of the 2nd ACM International Conference on Multimedia Retrieval*, Hong Kong, China, June 5 – 8, 2012, ISBN: 978-1-4503-1329-2, pp. 1–8, 2012, Published by ACM, DOI: 10.1145/2324796.2324850, Available: https://dl.acm.org/doi/10.1145/2324796.2324850.

[4] Anne-Marie Tousch, StePhane Herbin and Jean-Yves Audibert, "Semantic hierarchies for image annotation: A survey", *Pattern Recognition*, ISSN:0031-3203, Vol. 45, No. 1, pp. 333–345, January 2012, Published by Elsevier, DOI: 10.1016/j.patcog.2011.05.017, Available: https://www.sciencedirect.com/science/article/abs/pii/S0031320311002652.

[5] Ahmad Mueen, Roziati Zainuddin and Mohd Sapian Baba, "Automatic multilevel medical image annotation and retrieval", *Journal of Digital Imaging*, PMID:17846834, Vol. 21, No. 3, pp. 290–5, September 2008, Published by PMC, DOI: 10.1007/s10278-007-9070-3, Available: https://www.ncbi.nlm.nih.gov/pmc/articles/PMC3043841/.

[6] José Ramos, Thessa T.J.P. Kockelkorn, Isabel Ramos, Rui Ramos, Jan Grutters *et al.*, "Content-Based Image Retrieval by Metric Learning From Radiology Reports : Application to Interstitial Lung Diseases", *IEEE Journal of Biomedical and Health Informatics*, ISSN: 2168-2208, Vol. 20, No. 1, pp. 281–292, 2016, Published by IEEE, DOI: 10.1109/JBHI.2014.2375491, Available: https://ieeexplore.ieee.org/document/6966720.

[7] Hanwang Zhang, Zheng-Jun Zha, Yang Yang, Shuicheng Yan, Yue Gao *et al.*, "Attribute-Augmented Semantic Hierarchy: Towards a Unified Framework for Content-Based Image Retrieval", *ACM Transactions on Multimedia Computing, Communications, and Applications*, ISSN: 1551-6857, Vol. 11, No. 1s, pp. 21:1--21:21, October 2014, Published by ACM, DOI: 10.1145/2637291, Available: https://dl.acm.org/doi/abs/10.1145/2637291.

[8] Yimo Tao, Zhigang Peng, Arun Krishnan, and Xiang Sean Zhou, "Robust learning-based parsing and annotation of medical radiographs", *IEEE Transactions on Medical Imaging*, Electronic ISSN:1558-254X, Vol. 30, No. 2, pp. 338–50, Febuary 2011, Published by IEEE, DOI: 10.1109/TMI.2010.2077740, Available: https://ieeexplore.ieee.org/document/5586655.

[9] Donia Ben Hassen and Hassen Taleb, "Lesion detection in lung regions that are segmented using spatial relations", in *International Conference on Information Technology and e-Services*, Sousse, Tunisia, March 24-26, 2012, ISBN**:** 978-1-4673-1166-3, pp. 1–4, Published by IEEE, DOI: 10.1109/ICITeS.2012.6216669, Available: https://ieeexplore.ieee.org/document/6216669.

[10] Thanh Minh Nguyen and Qing Ming Jonathan Wu, "Robust student's-t mixture model with spatial constraints and its application in medical image segmentation", *IEEE Transactions on Medical Imaging*, Electronic ISSN:1558-254X, Vol. 31, No. 1, pp. 103–116, 2012, Published by IEEE, DOI: 10.1109/TMI.2011.2165342, Available: https://ieeexplore.ieee.org/document/5989867.

[11] Yang Song, Weidong Cai and Dagan Feng, "Hierarchical spatial matching for medical image retrieval", in *Proceedings of the 2011 International ACM workshop on Medical multimedia analysis and retrieval*, Scottsdale, Arizona, USA, November 26, 2011, ISBN:978-1-4503-0991-2, pp. 1–6, Published by ACM, DOI: 10.1145/2072545.2072547, Available: https://dl.acm.org/doi/10.1145/2072545.2072547.

[12] Parisa Kordjamshidi, Martijn Van Otterlo and Marie-Francine Moens, "Spatial Role Labeling: Towards Extraction of Spatial Relations from Natural Language", *ACM Transactions on Speech and Language Processing*, ISSN: 1550-4875, Vol. 8, No. 3, pp. 4:1-4:36, December 2011, Published by ACM, DOI: 10.1145/2050104.2050105, Available: https://dl.acm.org/doi/10.1145/2050104.2050105.

[13] Shaharyar Ahmed Khan Tareen and Hayat Muhammad Khan, "Novel Slope Detection and Calculation Techniques for Mobile Robots", in *2nd International Conference on Robotics and Artificial Intelligence*, Islamabad, Pakistan, November 1-2, 2016, ISBN: 978-1-5090-4060-5, Vol. 2, No. 1, pp. 158–163, Published by IEEE, DOI:

10.1109/ICRAI.2016.7791246, Available: https://ieeexplore.ieee.org/document/7791246.

[14] Hui Hui Wang, Daud Mohamad and Nor Azman Ismail, "An Efficient Parameters Selection for Object Recognition Based Colour Features in Traffic Image Retrieval", *International Arab Journal of Information Technology*, Online ISSN: 2309-4524, Vol. 11, No. 3, pp. 308–314, 2014, Available: https://www.iajit.org/PDF/vol.11,no.3/4719.pdf.

[15] Eliseo Clementini, "Directional relations and frames of reference", *Geoinformatica*, Electronic ISSN: 1573-7624, Vol. 17, No. 2, pp. 235–255, 2013, Published by Springer, DOI: 10.1007/s10707-011-0147-2, Available: https://link.springer.com/article/10.1007/s10707-011-0147-2.

[16] Biao Jin, Wenlong Hu and Hongqi Wang, "Human Interaction Recognition Based on Transformation of Spatial Semantics", *IEEE Signal Processing Letters*, Electronic ISSN: 1558-2361, Vol. 19, No. 3. pp. 139–142, 2012, Published by IEEE, DOI: 10.1109/LSP.2012.2183364, Available: https://ieeexplore.ieee.org/document/6125990.

[17] Laura Hollink, Guus Schreiber, Jan Wielemaker and Bob Wielinga, "Semantic annotation of image collections", *Knowledge Capture*, Vol. 2, 2003, Available: https://www.cs.vu.nl/~guus/papers/Hollink03b.pdf.

[18] Markus Schneider, Tao Chen, Ganesh Viswanathan and Wenjie Yuan, "Cardinal directions between complex regions", *ACM Transactions on Database Systems*, ISSN:0362-5915, Vol. 37, No. 2, 2012, Published by ACM, DOI: 10.1145/2188349.2188350, Available: https://dl.acm.org/doi/10.1145/2188349.2188350.

[19] Spiros Skiadopoulos, Christos Giannoukos, Nikos Sarkas, Panos Vassiliadis, Timos Sellis *et al.*, "Computing and Managing Cardinal Direction Relations", *IEEE Transactions on Knowledge and Data Engineering*, Electronic ISSN: 1558-2191, Vol. 17, No. 12, pp. 1610–1623, 2005, Published by IEEE, DOI: 10.1109/TKDE.2005.192, Available: https://ieeexplore.ieee.org/document/1524962.

[20] Tiberio Uricchio, Lamberto Ballan, Lorenzo Seidenari and Alberto Del Bimbo, "Automatic image annotation via label transfer in the semantic space", *Pattern Recognition*, Online ISSN: 1873-5142, Vol. 71, pp. 144–157, 2017, Published by Elsevier, DOI: 10.1016/j.patcog.2017.05.019, Available: https://www.sciencedirect.com/science/article/abs/pii/S0031320317302066.

[21] Dengsheng Zhang, Md Monirul Islam and Guojun Lu, "A review on automatic image annotation techniques", *Pattern Recognition*, Online ISSN: 1873-5142, Vol. 45, No. 1, pp. 346–362, Jan. 2012, Published by Elsevier, DOI: 10.1016/j.patcog.2011.05.013, Available: https://www.sciencedirect.com/science/article/abs/pii/S0031320311002391.

[22] Claudio Carpineto and Giovanni Romano, "A Survey of Automatic Query Expansion in Information Retrieval", *ACM Computing Surveys*, ISSN: 0360-0300, Vol. 44, No. 1, pp. 1–50, January 2012, Published by ACM, DOI: 10.1145/2071389.2071390, Available: https://dl.acm.org/doi/10.1145/2071389.2071390.

[23] Xianhua Zeng, Shiyue Tong, Yuzhe Lu, Liming Xu and Zhiwei Huang, "Adaptive Medical Image Deep Color Perception Algorithm", *IEEE Access*, Electronic ISSN**:** 2169-3536, Vol. 8, pp. 56559–56571, 2020, Published by IEEE, DOI: 10.1109/ACCESS.2020.2982187, Available: https://ieeexplore.ieee.org/document/9043495.

[24] Bram Van Ginneken, Alejandro F. Frangi, Joes Staal, Bart M. ter Haar Romeny and Max A. Viergever, "Active Shape Model Segmentation With Optimal Features", *IEEE Transactions on Medical Imaging*, Electronic ISSN: 1558-254X, Vol. 21, No. 8, pp. 924–933, 2002, Published by IEEE, DOI: 10.1109/TMI.2002.803121, Available: https://ieeexplore.ieee.org/document/1076037.

[25] Ashfaq Hussain and Ajay Khunteta, "Semantic Segmentation of Brain Tumor from MRI Images and SVM Classification using GLCM Features", *Proceedings of the 2nd International Conference on Inventive Research in Computing Applications*, Coimbatore, India, July 15-17, 2020, Electronic ISBN**:** 978-1-7281-5374-2, pp. 38–43, DOI: 10.1109/ICIRCA48905.2020.9183385, Available: https://ieeexplore.ieee.org/document/9183385.

[26] Ritendra Datta, Dhiraj Joshi, Jai Li and James Ze Wang, "Image retrieval: Ideas, influences, and trends of the new age", *ACM Computing Surveys*, ISSN:0360-0300, Vol. 40, No. 2, pp. 1–60, April 2008, Published by ACM, DOI: 10.1145/1348246.1348248, Available: https://dl.acm.org/doi/10.1145/1348246.1348248.

[27] Qimin Cheng, Qian Zhang, Peng Fu, Conghuan Tu and Seng Li, "A survey and analysis on automatic image annotation", *Pattern Recognition*, Online ISSN: 1873-5142, Vol. 79, pp. 242–259, June 2018, DOI: 10.1016/j.patcog.2018.02.017, Available: https://www.sciencedirect.com/science/article/abs/pii/S0031320318300670.

[28] Luca Piras and Giorgio Giacinto, "Information fusion in content based image retrieval: A comprehensive overview", *Information Fusion*, Online ISSN: 1872-6305, Vol. 37, pp. 50–60, 2017, Published by Elsevier, DOI: 10.1016/j.inffus.2017.01.003, Available: https://www.sciencedirect.com/science/article/abs/pii/S1566253517300076.

[29] Mohd Nizam Saad, Zurina Muda, Noraidah Sahari Ashaari, Hamzaini Abdul Hamid and Nur Hhasanan binti Abdul Hasan, "The spatial relation features for describing objects relationships within image", in *International Conference on Electrical Engineering and Informatics*, Denpasar, Indonesia, August 10-11, 2015, Electronic ISBN**:**978-1-4673-7319-7, pp. 126–131, Published by IEEE, DOI: 10.1109/ICEEI.2015.7352482, Available: https://ieeexplore.ieee.org/document/7352482.

[30] Hanbo Zhang, Xuguang Lan, Xinwen Zhou, Zhiqiang Tian, Yang Zhang *et al.*, "Visual manipulation relationship recognition in object-stacking scenes", *Pattern Recognition Letters*, Online ISSN: 1872-7344, Vol. 140, pp. 34–42, 2020, Published by Elsevier, DOI: 10.1016/j.patrec.2020.09.014, Available: https://www.sciencedirect.com/science/article/abs/pii/S0167865520303445.

[31] Xioming Zhou, Chuan Heng Ang and Tok Wang Ling, "Image retrieval based on object's orientation spatial

relationship", *Pattern Recognition Letters*, ISSN: 1872-7344, Vol. 22, No. 5, pp. 469–477, 2001, DOI: 10.1016/S0167-8655(00)00123-9, Available: https://www.sciencedirect.com/science/article/abs/pii/S0167865500001239.

[32] Max J. Egenhofer and Robert D. Franzosa, "Point-set topological spatial relations", *International Journal of Geographical Information Systems*, Online ISSN: 1362-3087, Vol. 5, No. 2, pp. 161–174, January 1991, Published by Taylor & Francis Online, DOI: 10.1080/02693799108927841, Available: https://www.tandfonline.com/doi/abs/10.1080/02693799108927841.

[33] Max J. Egenhofer, Jayaht Sharma and David M. Mark, "A Critical Comparison of the 4-Intersection and 9-Intersection Models for Spatial Relations: Formal Analysis", in *Proceedings of the Eleventh International Symposium on Computer-Assisted Carthography (Auto-Carto 11)*, ISBN:1-57083-001-0, No. 92, 1993, Available: http://www.dpi.inpe.br/gilberto/references/max_comparison_4_9_intersection.pdf.

[34] Micheal Grüninger and Bahar Aameri, "A new perspective on the mereotopology of RCC8", in *Leibniz International Proceedings in Informatics*, L'Aquila, Italy, September 4-8, 2017, ISBN: 978-3-319-63946-8, Vol. 86, No. 2, pp. 1–2, DOI: 10.4230/LIPIcs.COSIT.2017.2, Available: https://drops.dagstuhl.de/opus/volltexte/2017/7757/pdf/LIPIcs-COSIT-2017-2.pdf.

[35] Juan Chen, Anthony G. Cohn, Dayou Liu, Shengsheng Wang, Jihong Ouyang *et al.*, "A Survey of Qualitative Spatial Representations", *Knowledge Engineering Review*, ISSN: 0269-8889, Vol. 30, No. 1, pp. 106–136, 2013, DOI: https://doi.org/10.1017/S0269888913000350, Available: https://eprints.whiterose.ac.uk/83881/1/KER521.pdf.

[36] Frank Dylla, Jae Hee Lee, Till Mossakowski, Thomas Schneider, André Van Delden *et al.*, "A Survey of Qualitative Spatial and Temporal Calculi", *ACM Computing Surveys*, ISSN:0360-0300, Vol. 50, No. 1, pp. 1–39, 2017, Published by ACM, DOI: 10.1145/3038927, Available: https://dl.acm.org/doi/10.1145/3038927.

[37] Céline Hudelot, Jamal Atif and Isabelle Bloch, "Fuzzy spatial relation ontology for image interpretation", *Fuzzy Sets and Systems*, Online ISSN: 1872-6801, Vol. 159, No. 15, pp. 1929–1951, August 2008, Published by Elsevier, DOI: 10.1016/j.fss.2008.02.011, Available: https://www.sciencedirect.com/science/article/abs/pii/S0165011408001012.

[38] John Freeman, "The modelling of spatial relations", *Computer Graphics and Image Processing*, ISSN: 0146-664X, Vol. 4, No. 2, pp. 156–171, June 1975, Published by Elsevier, DOI: 10.1016/S0146-664X(75)80007-4, Available: http://linkinghub.elsevier.com/retrieve/pii/S0146664X75800074.

[39] Cristian Landsiedel, Verena Rieser, Matthew Walter and Dirk Wollherr, "A review of spatial reasoning and interaction for real-world robotics", *Advanced Robotics*, Online ISSN: 1568-5535, Vol. 31, No. 5, pp. 222–242, 2017, Published by Taylor & Francis Online, DOI: 10.1080/01691864.2016.1277554, Available: https://www.tandfonline.com/doi/abs/10.1080/01691864.2016.1277554.

[40] Zhongyi Xie, W. Randolph Franklin and Daniel M. Tracy, "Ph.D. Showcase: Slope Preserving Lossy Terrain Compression", *SIGSPATIAL Special*, Electronic ISSN:1946-7729, Vol. 2, No. 3, pp. 19–24, 2010, Published by ACM, DOI: 10.1145/1953102.1953106, Available: https://dl.acm.org/doi/pdf/10.1145/1953102.1953106.

[41] Frank Duque, Ruy Fabila-Monroy and Carlos Hidalgo-toscano, "Point Sets with Small Integer Coordinates and no Large Convex Polygons", *Discrete and Computational Geometry*, Electronic ISSN: 1432-0444, Vol. 59, pp. 461–476, 2018, Published by Springer, DOI: 10.1007/s00454-017-9931-6, Available: https://link.springer.com/article/10.1007/s00454-017-9931-6.

[42] Hui Hui Wang, Dzulkifli Mohamad and Norazman Ismail, "Semantic Gap in CBIR: Automatic Objects Spatial Relationships Semantic Extraction and Representation", *International Journal of Image Processing*, ISSN: 1985-2304, No. 4, pp. 192–204, 2010, Available: http://www.cscjournals.org/csc/manuscript/Journals/IJIP/volume4/Issue3/IJIP-189.pdf.

[43] Anthony Cohn, Sanjiang Li, Weiming Liu and Jochen Renz, "Reasoning about Topological and Cardinal Direction Relations Between 2-Dimensional Spatial Objects", *Journal of Artificial Intelligence Research*, ISSN: 1076 – 9757, Vol. 51, pp. 493–532, 2014, DOI: 10.1613/jair.4513, Available: https://www.jair.org/index.php/jair/article/view/10914/26023.

[44] Sangha Nam and Incheol Kim, "Qualitative spatial reasoning with directional and topological relations", *Mathematical Problems in Engineering*, Online ISSN: 1563-5147, Vol. 2015, 2015, Published by Hindawi, DOI: 10.1155/2015/902043, Available: https://www.hindawi.com/journals/mpe/2015/902043/.

[45] Jingwei Shen, Dongzhe Zhao, Kaifang Shi and Mingguo Ma, "A model for representing topological relations between lines considering metric details", *Journal of Geographical Systems*, Electronic ISSN: 1435-5949, Vol. 23, pp. 407–424, 2021, DOI: 10.1007/s10109-021-00355-5. Available: https://link.springer.com/article/10.1007/s10109-021-00355-5.

[46] Laura Hollink, Giang Nguyen, Guus Schreiber, Jan Wielemaker and Marcel Worring, "Adding Spatial Semantics to Image Annotations", in *Proceedings of the 4th International Workshop on Knowledge Markup and Semantic Annotation 2004 (SemAnnot 2004)*, 8th November 2004, Hiroshima, Japan, pp. 31-40, Available: https://ceur-ws.org/Vol-184/semAnnot04-04.pdf.

[47] Bryan C. Russell, Antonio Torralba, Kevin P. Murphy and William T. Freeman, "LabelMe: A Database and Web-Based Tool for Image Annotation", *International Journal of Computer Vision*, Electronic ISSN:1573-1405, Vol. 77, No. 1–3, pp. 157–173, October 2008, DOI: 10.1007/s11263-007-0090-8, Available:

https://people.csail.mit.edu/brussell/research/AIM-2005-025-new.pdf.

[48] Mohd Nizam Saad, Zurina Muda, Noraidah Sahari and Hamzaini Abdul Hamid, "Multiclass classification for chest x-ray images based on lesion location in lung zones", *Journal of Telecommunication, Electronic and Computer Engineering*, Electronic ISSN: 2289-8131, Vol. 9, No. 1–2, pp. 19–23, 2017, Available: https://jtec.utem.edu.my/jtec/article/view/1644.

[49] Nigel Chapman and Jenny Chapman, *Digital Multimedia*, ISBN: 978-0-470-51216-6, 3rd ed. Sussex, UK: John Wiley & Sons, 2009.